ground water

A Nested-Cell Approach for In Situ Remediation

by Jian Luo[1,4], Weimin Wu[1], Michael N. Fienen[1], Philip M. Jardine[2], Tonia L. Mehlhorn[2], David B. Watson[2], Olaf A. Cirpka[3], Craig S. Criddle[1], and Peter K. Kitanidis[1]

Abstract

We characterize the hydraulics of an extraction-injection well pair in arbitrarily oriented regional flow by the recirculation ratio, area, and average residence time in the recirculation zone. Erratic regional flow conditions may compromise the performance of the reactor between a single well pair. We propose an alternative four-well system: two downgradient extraction and two upgradient injection wells creating an inner cell nested within an outer cell. The outer cell protects the inner cell from the influence of regional flow. Compared to a two-well system, the proposed four-well system has several advantages: (1) the recirculation ratio within the nested inner cell is less sensitive to the regional flow direction; (2) a transitional recirculation zone between the inner and outer cells can capture flow leakage from the inner cell, minimizing the release of untreated contaminants; and (3) the size of the recirculation zone and residence times can be better controlled within the inner cell by changing the pumping rates. The system is applied at the Field Research Center in Oak Ridge, Tennessee, where experiments on microbial in situ reduction of uranium (VI) are under way.

Introduction

In situ bioremediation of contaminated ground water often involves delivery of an electron donor or acceptor and nutrients into the aquifer to create a biologically active zone in which bacteria are stimulated to transform the contaminants. Effective chemical delivery is recognized as a critical issue in the design of such systems. The reactants must mix with the contaminant to facilitate microbial growth and biodegradation (Sturman et al. 1995; Dybas et al. 1998; Witt et al. 1999; Hyndman et al. 2000). Extraction and injection wells create recirculation zones functioning as in situ reactors and may provide a high degree of hydraulic control. This setup is effective in delivering and mixing dissolved compounds and has been successfully applied for in situ bioremediation (McCarty et al. 1998; Hyndman et al. 2000; Gandhi et al. 2002).

In pump-and-treat applications, the objective is to optimize the number, location, and flow rates of wells to capture the plume reliably and with minimal effort (Gorelick et al. 1993). Designing in situ reactors includes additional design criteria, such as the recirculation ratio, i.e., the proportion of flow within the recirculation zone to the well flow rate, the area or volume of the recirculation zones, and the residence-time distribution within the recirculation zones. Christ et al. (1999) present a semianalytical scheme to evaluate the recirculation ratio of flow within recirculation zones created by multiple colinear well pairs. Cunningham and Reinhard (2002) compared the hydraulics of an injection-extraction well pair and permeable reactive barriers, focusing on capture zone width, assuming the regional flow direction is orthogonal to the well placement. Zhan (1999), Luo and Kitanidis (2004), and Cunningham et al. (2004) present analytical and semianalytical results for the fluid residence time within the recirculation zone.

The present work was motivated by the need to create an in situ reactor to investigate the microbial reduction of mobile and soluble U(VI) to immobile and insoluble U(IV) in a highly acidic nitrate-contaminated aquifer in Oak Ridge, Tennessee. The contamination

[1]Department of Civil & Environmental Engineering, Stanford University, Stanford, CA 94305-4020.
[2]Environmental Science Division, Oak Ridge National Laboratory, Oak Ridge, TN 37831-6038.
[3]Swiss Federal Institute for Environmental Science and Technology (EAWAG), Überlandstr. 133, 8600 Dübendorf, Switzerland.
[4]Corresponding author: (650) 723-1825; fax (650) 725-9720; jianluo@stanford.edu
Received September 2004, accepted March 2005.

doi: 10.1111/j.1745-6584.2005.00106.x

conditions complicate the hydraulic control requirements for the in situ reactor design. The performance must be unaffected by regional flow conditions, release of untreated uranium to downgradient areas must be minimized, and the residence-time distribution within the in situ reactor must be conveniently adjusted.

We consider two-dimensional ground water flow in a homogeneous, isotropic aquifer. We first analyze the two-dimensional hydraulics of the recirculation zone created by a single-reactor system with an extraction-injection well pair with arbitrarily oriented regional flow. We consider the recirculation ratio, the area of the recirculation zone, and the average residence time within the recirculation zone. Then, we propose a nested-cell design, consisting of two upgradient injection wells and two downgradient extraction wells. We show that in the inner cell the recirculating flow is less influenced by the regional flow than a single well pair and leakage may be captured by the outer cell. This design was applied in the experiment on uranium bioreduction in Oak Ridge, Tennessee. We evaluate the hydraulic performance of the nested inner cell design based on tracer test data.

Single-Reactor System

We implement and extend the approach of Luo and Kitanidis (2004) to analyze the single-reactor system. Parameters and variables listed in Table 1 are used to calculate the flow field. The origin of the system of coordinates is chosen as the midpoint between the two wells, which are placed on the x-axis with spacing $2d$. The spatial coordinates are made dimensionless by dividing by d. The regional flow Q_0 is oriented at angle α from the x-axis. The pumping rate is Q_w. Aquifer porosity is n, and uniform thickness is b.

Recirculation Ratio

The recirculation ratio, P_r, is the total volumetric flux between the wells divided by the pumping rate (Luo and Kitanidis 2004):

$$P_r = 1 - \frac{|\Psi_{sd}|}{\pi\lambda} \tag{1}$$

where $|\Psi_{sd}|$ is the absolute value of the dimensionless stream function at the stagnation points and λ is the dimensionless pumping rate. The capture ratio, P_c, is defined as the normalized regional flow captured by the extraction well:

$$P_c = 1 - P_r = \frac{|\Psi_{sd}|}{\pi\lambda} \tag{2}$$

Figure 1 shows the recirculation and capture ratios for a single well pair as a function of regional flow orientation for dimensionless pumping rate $\lambda = 10$. P_r and P_c are sensitive to the regional flow orientation. At $\alpha = 0$, P_r reaches the maximum value of unity, indicating complete recirculation between the injection and extraction wells. Changing the α, P_r decreases and P_c increases until $\alpha = \pi$, where the extraction well is directly upgradient of the injection well. Although in real aquifers perfect recirculation never occurs because heterogeneity distorts the flow field, this analysis highlights the effect of regional flow orientation.

Figure 2 shows that the recirculation ratio P_r increases and the capture ratio P_c decreases with the pumping rate λ. The effect of changing λ is more prominent when λ is small. To reach a certain recirculation ratio, the required λ depends on α. Under certain circumstances, a recirculation zone and a capture/release zone are not both possible. For

Table 1
Parameters and Variables for the Characterization of the Single-Reactor Flow Field

Symbol	Description	Nondimensionlization
x, y, z	Coordinates [L]	$x_d = x/d$, $y_d = y/d$, $z_d = x_d + iy_d$
Q_0	Regional flow rate [$L^2\ T^{-1}$]	$Q_{0d} = e^{i\alpha}$
Q_w	Well pumping rate [$L^3\ T^{-1}$]	$\lambda = \dfrac{Q_w}{2\pi Q_0 d}$
Q_R	Recirculation flow rate [$L^3\ T^{-1}$]	$P_r = Q_R/Q_w$
Ω	Complex potential [$L^3\ T^{-1}$]	$\Omega_d = \lambda \ln\left(\dfrac{z_d - 1}{z_d + 1}\right) - z_d e^{-i\alpha}$
Φ	Discharge potential [$L^3\ T^{-1}$]	$\Phi_d = \dfrac{\lambda}{2} \ln\left[\dfrac{(x_d-1)^2 + y_d^2}{(x_d+1)^2 + y_d^2}\right] - (x_d \cos\alpha + y_d \sin\alpha)$
Ψ	Stream function [$L^3\ T^{-1}$]	$\Psi_d = \lambda(\theta_1 - \theta_2) - (y_d \cos\alpha - x_d \sin\alpha)$, where $\theta_1 = \tan^{-1}\left(\dfrac{y_d}{x_d - 1}\right)$, $\theta_2 = \tan^{-1}\left(\dfrac{y_d}{x_d + 1}\right)$
A	Area of the recirculation zone [L^2]	$A_d = A/d^2$
t_R	Average residence time within the recirculation zone, $t_R = \dfrac{nAb}{Q_R}$ [T]	$\tau_R = \dfrac{t_R}{T} = \dfrac{A_d}{P_r \lambda}$, where $T = \dfrac{nbd}{2\pi Q_0}$

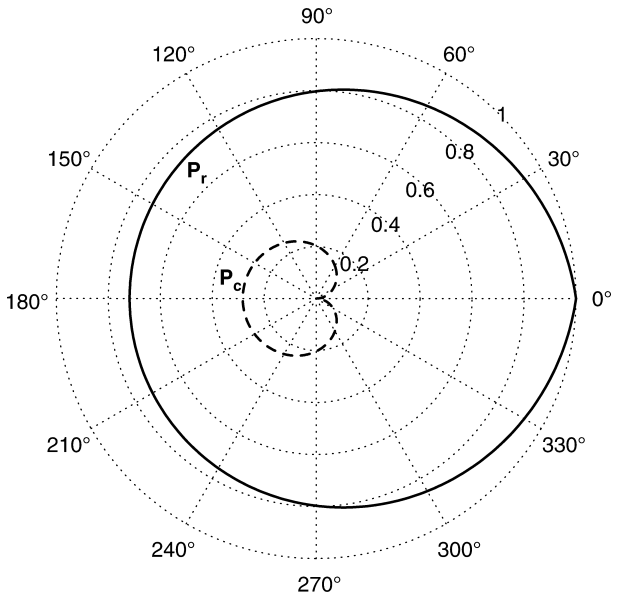

Figure 1. Recirculation ratio (P_r) and capture ratio (P_c) for an extraction-injection well pair as a function of regional flow orientation α. Dimensionless pumping rate $\lambda = 10$.

example, for $\alpha = 0$, there are no capture and release zones. For $\alpha \neq 0$, a minimum pumping rate, λ_{min}, must be exceeded to guarantee recirculation. Its value is given by $P_r = 0$, i.e., $|\Psi_{sd}| = \pi\lambda_{min}$, which is the stream function value at the origin. Thus, in this critical case the separation streamline passes through the stagnation points and the origin, regardless of the regional flow orientation, and divides the flow field into a capture zone and a release zone but no recirculation zone exists. For $\alpha = 0$, full recirculation is achieved for any nonzero pumping rate. If the well placement is parallel to the regional flow with an upgradient extraction well and a downgradient injection well, i.e., $\alpha = \pi$, $\lambda_{min} = 1/2$. At $\alpha = \pi/2$, $\lambda_{min} = 0.5495$, which is consistent with Cunningham and Reinhard (2002). The maximum value of λ_{min} is ~0.6366 reached at $\alpha \approx 130°$. Thus, if $\lambda > 0.6333$, a recirculation zone will exist regardless of regional flow orientation.

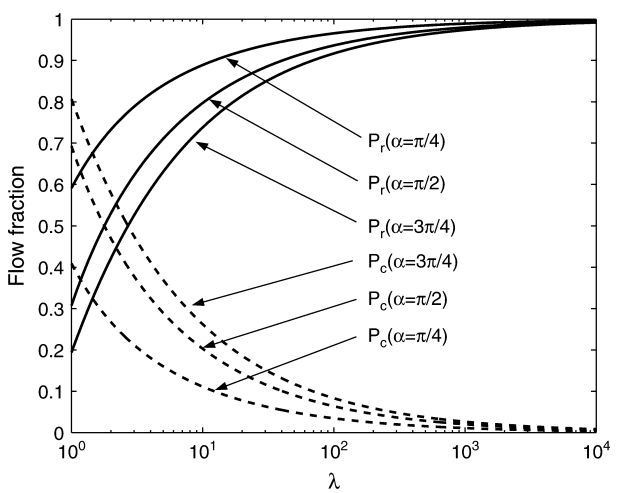

Figure 2. Recirculation ratio (P_r) and capture ratio (P_c) as a function of the dimensionless pumping rate (λ).

Average Residence Time

The average residence time, t_R, is the reactor volume divided by the discharge. Figure 3 shows that the dimensionless area and the average residence time within the recirculation zone depend similarly on regional flow orientation because A_d is much more sensitive to α than the recirculation ratio P_r, so that the ratio $A_d/P_r = \lambda\tau_R$ is dominated by the behavior of A_d. The largest residence time τ_R is found for the perfect recirculation pair ($\alpha = 0$), which creates the largest recirculation zone, and the smallest is for the injection well directly downgradient of the extraction well ($\alpha = \pi$), which creates the smallest recirculation zone.

Figure 4a shows that the dimensionless recirculation area A_d depends linearly on the pumping rate λ with different slopes for different α. The slope is between 1.735 and 2π. The maximum and minimum are reached at $\alpha = 0$ and $\alpha = \pi$, respectively. P_r is 1 at $\alpha = 0$, so τ_R becomes a constant, 2π (Luo and Kitanidis 2004). For other regional flow directions, increasing λ affects τ_R only when $\lambda < 20$ because increasing the pumping rate λ makes the recirculation ratio P_r approach unity quickly, resulting in $\tau_R \rightarrow A_d/\lambda$. Thus for large λ, the increase in λ and the linear increase in A_d cancel each other in the evaluation of τ_R (Figure 4b). The dimensional residence time is:

$$t_R = \tau_R T = \tau_R \frac{nbd}{2\pi Q_0} \tag{3}$$

Thus, increasing pumping rates is not an effective way to change the residence time within the recirculation zone in the range of $\lambda > 20$.

Nested Inner Cell

In many applications, we need to create a well-controlled recirculation zone, separated from the regional

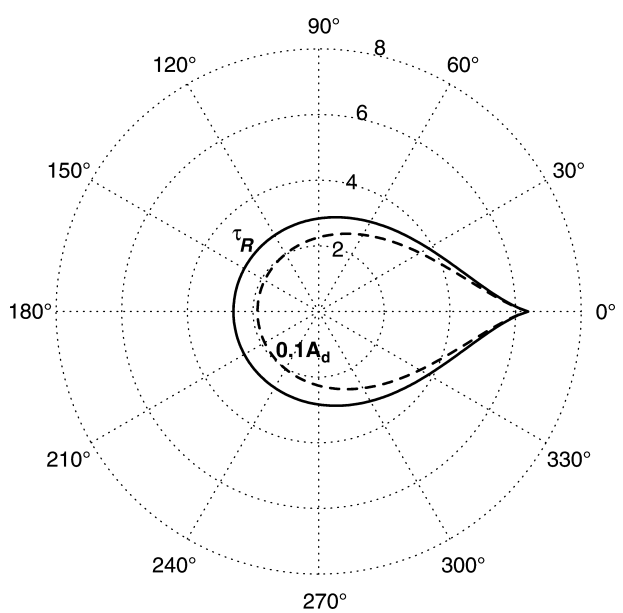

Figure 3. Dimensionless area, A_d, and average dimensionless residence time, τ_R, within the recirculation zone created by an extraction-injection well pair at $\lambda = 10$ as a function of α. The dashed line represents 0.1 A_d, and the solid line represents τ_R.

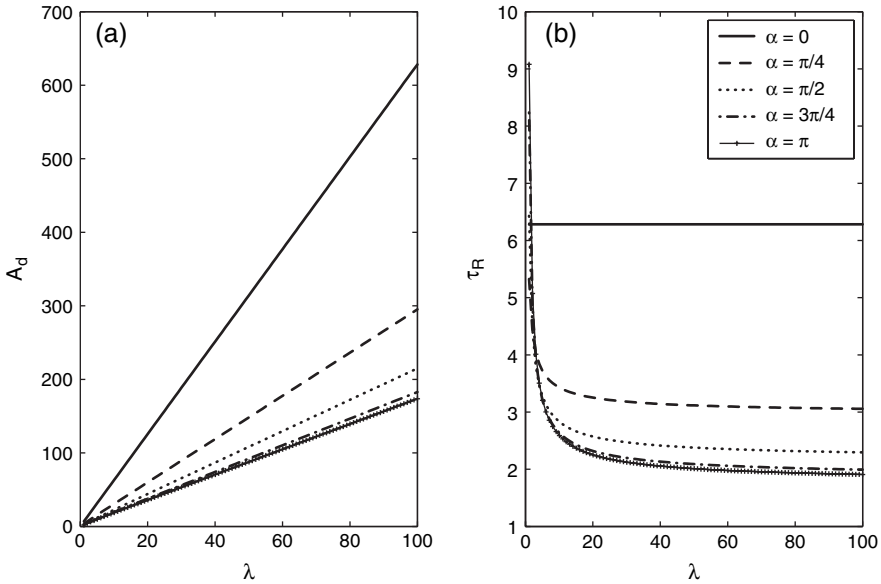

Figure 4. Dimensionless area (A_d) and average residence time (τ_R) within the recirculation zone as a function of the dimensionless pumping rate (λ). (a) A_d; (b) τ_R.

flow, i.e., $P_r = 1$. In theory, this requirement could be met by a two-well system where the wells are perfectly aligned with the regional flow ($\alpha = 0$). Such a system would create a closed loop, where all the water injected moves to the extraction well and the regional flow does not pass through either well. In practice, however, the direction of regional flow may be unknown and vary with time, making complete recirculation unrealistic in field applications.

Here, we propose a four-well system as depicted in Figure 5. Two injection wells are placed upgradient, and two extraction wells are placed downgradient. In the ideal case, regional flow is parallel to the well alignment and four stagnation points are located on the x-axis of the system of chosen coordinates. Two stagnation points are between the inner and outer well pairs, and the other two are located outside of the outer well pair. Streamlines passing through the stagnation points delineate two "closed loops." An inner cell is enclosed by an outer cell and thereby separated from regional flow. To compare the hydraulic performance of the nested cell with the single-reactor system, we assume the wells have identical flow rates of $\pm Q_w/2$, so the total pumping rate of the four-well system equals that of the two-well system. The spacings between the inner wells and outer wells are $2d$ and $4d$, respectively. We use the same dimensionless variables as for the previous system.

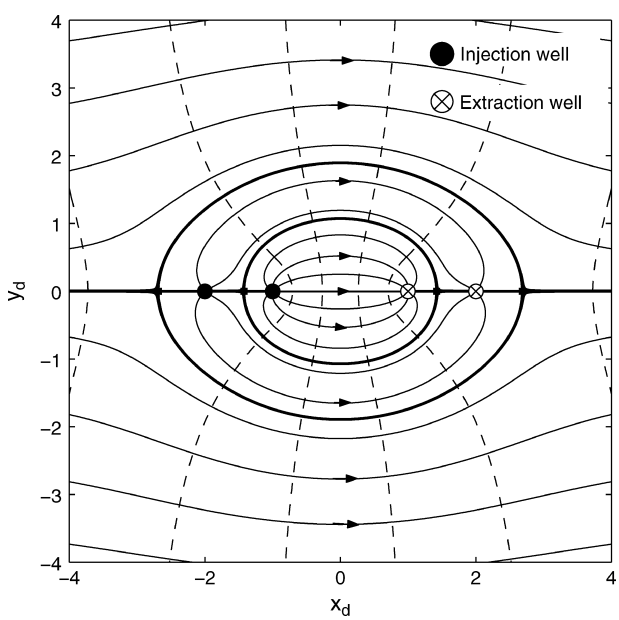

Figure 5. Flow net created by an ideal four-well system. Solid lines: streamlines; dashed lines: equipotential lines; bold solid lines: separation streamlines.

Recirculation Ratio

The four-well system has four stagnation points:

$$z_{sd}^2 = \frac{5}{2} + \frac{3}{2}\lambda e^{i\alpha} \pm \frac{1}{2}\sqrt{9\lambda^2 e^{i2\alpha} + 6\lambda e^{i\alpha} + 9} \qquad (4)$$

The recirculation ratios for the inner and outer cells in the four-well system are given by:

$$P_r^{inner} = 2 - \frac{2|\Psi_{sd}^{inner}|}{\pi\lambda}$$
$$P_r^{outer} = 1 - \frac{|\Psi_{sd}^{outer}|}{\pi\lambda} \qquad (5)$$

where Ψ_{sd}^{inner} and Ψ_{sd}^{outer} are the stream functions at the inner and outer cell stagnation points, respectively.

Figure 6 shows the recirculation ratio for both systems as a function of regional flow orientation for a dimensionless pumping rate of $\lambda = 10$. For the two-well system, the recirculation ratio P_r is unity only when regional flow is parallel to the well alignment ($\alpha = 0$). A deviation of 4° leads to a decrease of the recirculation

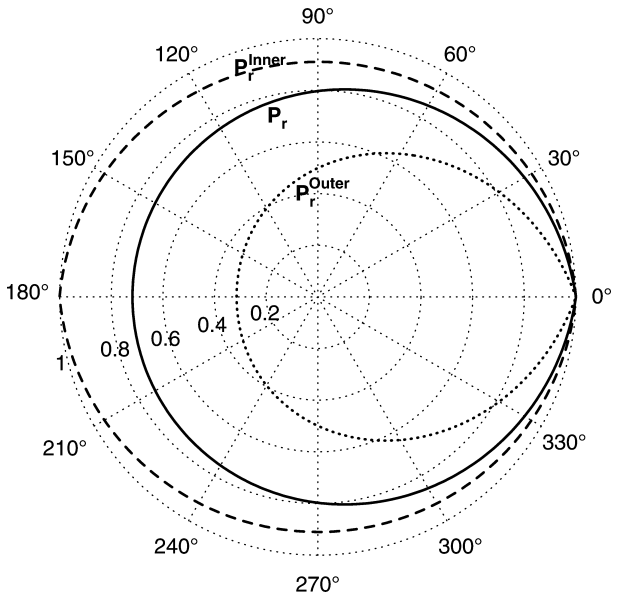

Figure 6. Recirculation ratio for the two-well and four-well systems as a function of the direction of regional flow at λ = 10. P_r, and P_r^{inner} and P_r^{outer} represent the recirculation ratios of the two-well system, and the inner and outer cells of the four-well system, respectively.

ratio to 99%, that is, 1% of the extracted water comes from the regional flow and 1% of the injected water is released to the ambient flow. At $\alpha = 30°$, P_r drops to 92.5%, and at $\alpha = 90°$, it drops to 80%. In contrast, the regional flow orientation has a smaller influence on the recirculation ratio of the nested inner cell created by the four-well system. P_r^{inner} is 99% at $\alpha = 7°$, 95.6% at $\alpha = 30°$, and 91% at $\alpha = 90°$. Thus, for the inner well pair, most flow recirculates in the inner cell regardless of the direction of regional flow, while the outer cell is more sensitive to the direction of regional flow than the recirculation zone of the two-well system because the inner cell distorts the outer cell streamlines (Figure 7).

Figure 7 shows the flow nets created by the two systems with regional flow orientation $\alpha = 30°$ and dimensionless pumping rate $\lambda = 10$. The flow field of the two-well system (Figure 7a) can be divided into four zones: capture zone, recirculation zone, release zone, and regional flow zone. About 92.5% of the pumped water circulates within the recirculation zone. From regional flow, 7.5% of the extracted water is captured, and the same amount is released from the injection well to regional flow. The flow field of the four-well system (Figure 7b) is more complicated. Three recirculation zones are identified: outer recirculation cell (zone I), inner recirculation cell (zone II), and between them a narrow recirculation zone (zone III) connecting the inner and outer well pairs. Water extracted by the outer extraction well includes recirculated water from zones I and III, and captured water from the regional flow. Water extracted by the inner extraction well includes the recirculated flow from zones II and III. The inner recirculation zone (zone II) is nested by zones I and III and has no direct connection to the regional flow.

Figure 8 shows the dependence of recirculation ratios P_r, P_r^{inner}, and P_r^{outer} on the dimensionless pumping rate λ. Increasing λ increases the recirculation ratios within the recirculation zones because the relative impact of regional flow decreases with higher pumping rates. However, to achieve a recirculation ratio larger than 85%, the two-well system requires a considerably higher pumping rate than the nested inner cell. Specifically, if nearly complete recovery is desired, i.e., $P_r > 0.99$, the pumping rate of the two-well system must be ~10 times larger than for the nested inner cell for $\alpha = 30°$. For large λ, the outer cell creates a flow field, which is almost parallel to the orientation of the inner wells, that is, the inner-cell flow field approaches a state similar to the two-well system at $\alpha = 0$. This also explains why the inner recirculation ratio approaches unity not only for $\alpha = 0$ but also for $\alpha = \pi$ (Figure 6).

Fluid Residence Times

Figure 9 shows the dimensionless area of the inner cell A_d^{inner} as a function of the dimensionless pumping rate λ. After a rapid initial increase, A_d^{inner} approaches an asymptotic value. This is very different from the single-

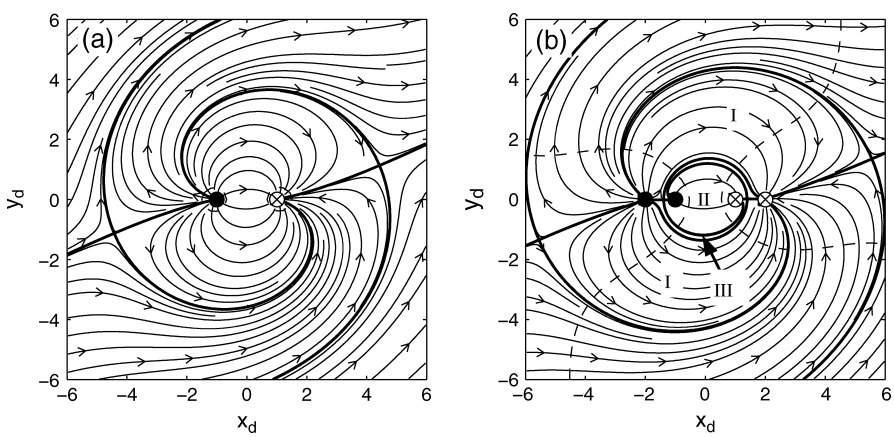

Figure 7. Flow nets at λ = 10, α = 30. Solid lines are streamlines, dashed lines are equipotential lines, and dark solid lines are separation streamlines. Arrows indicate the flow direction. (a) two-well system; (b) four-well system. Roman numerals refer to zones identified in the text.

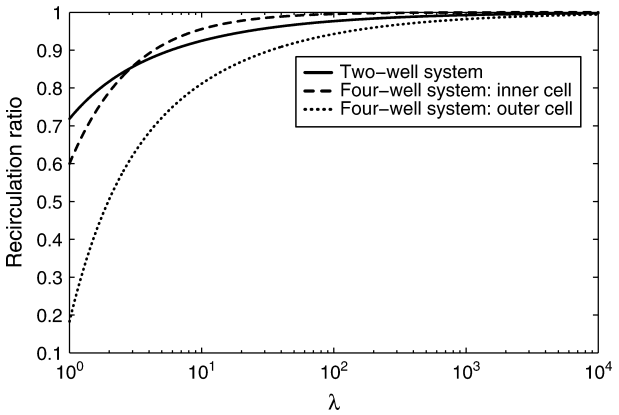

Figure 8. Recirculation ratios for the different setups as a function of the dimensionless pumping rate (λ). Orientation of regional flow, $\alpha = 30°$.

reactor system (Figure 4a), where A_d depends linearly on λ. The asymptotic value can be derived using Equation 4. At $\alpha = 0$,

$$z_{sd}^2 = \frac{5}{2} + \frac{3}{2}\lambda \pm \frac{1}{2}\sqrt{(3\lambda+1)^2 + 8} = \frac{5}{2} + \frac{3}{2}\lambda \pm \frac{1}{2}(3\lambda+1),\ \lambda \to \infty \quad (6)$$

Thus, the inner two stagnation points are given by:

$$z_{sd}^{inner} = \pm\sqrt{2} \quad (7)$$

When λ is large, the shape of the inner cell is circular with maximum area:

$$A_{max}^{inner} = 2\pi d^2, A_{d,max}^{inner} = 2\pi \quad (8)$$

In the previous section, we showed that it is difficult to change the average residence time within the recirculation zone of the two-well system once the wells are

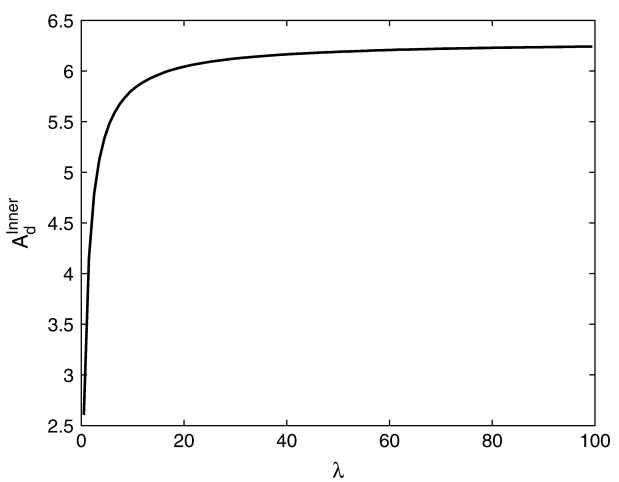

Figure 9. Dimensionless area of the inner cell as a function of the dimensionless pumping rate (λ). Orientation of regional flow, $\alpha = 0$.

installed because the area of the recirculation zone increases almost linearly with the pumping rate, particularly when α is close to zero. In contrast, the nested inner cell created by the four-well system approaches an asymptotic area (Equation 8), which makes it easy to adjust the average residence time within the inner cell by changing the pumping rates of the well. For $\lambda > 20$, we have:

$$t_R = \frac{4\pi d^2}{Q_w} \quad (9)$$

Thus, the average residence time within the inner cell becomes inversely proportional to the pumping rate if $\lambda > 20$. Furthermore, the flow field in the inner nested cell is more uniform than that of the two-well system, so the distribution of well-to-well travel time is more peaked and exhibits less tailing, meaning more uniform delivery of reactants into the treatment zone.

Application at Oak Ridge, Tennessee

We apply the proposed four-well system at the Field Research Center of the U.S. Department of Energy Natural and Accelerated Bioremediation program in Oak Ridge, Tennessee. The ground water at the site is acidic (pH ≈ 3.4), contains high levels of nitrate (≈10 g/L), and has high concentrations of metals. Soluble uranium is present at toxic levels of 20 to 50 mg/L. The general strategy proposed for stabilizing the contaminants within the aquifer is based on microbial reduction of U(VI), which is comparably mobile, to U(IV), which forms practically insoluble uraninite precipitates.

Full hydraulic control is essential in the design of the bioremediation experiment, which proceeds as follows. First, nitrate and calcium, which inhibit uranium bioreduction (Abdelouas et al. 1998; Senko et al. 2002; Finneran et al. 2002; Brooks et al. 2003), are washed out by an acidic, aluminum-free solution. Then, pH is raised to near-neutral conditions, which are favorable for U(VI)-reducing bacteria. Finally, ethanol is added as an electron donor to stimulate microbial activity. While the dissolved uranium is washed out in the first step, ~95% of the uranium remains in the system because it is sorbed to the soil matrix. It is crucial to keep ambient flow from entering the treatment zone because even 1% of high-nitrate water leakage could inhibit bioreduction of uranium. Furthermore, uranium mobilized at intermediate times must not be released to the downgradient regional flow.

We selected the four-well design proposed in the previous section to create favorable conditions for the uranium bioremediation experiment. Four pumping wells and three multilevel-sampling (MLS) wells were installed, all to 15 m depth (Figure 10). The pumping wells were intended to be aligned along strike, which is the x-axis in Figure 10. The MLS wells should have been aligned along dip, which is the y-axis in the figure. Regional flow is assumed oriented along strike with a hydraulic gradient <0.001. It is unrealistic to assume perfectly straight borehole installation when drilling in actual geologic media, and Figure 10 shows that the wells are not exactly aligned. The misalignment is due

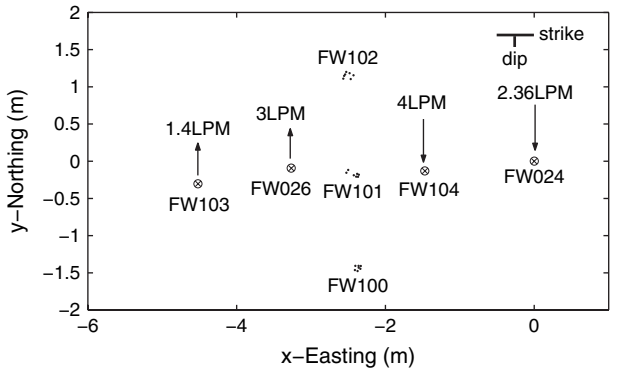

Figure 10. Plan view of the multiple-well system installed at Oak Ridge, Tennessee. FW024, outer injection well; FW104, inner injection well; FW026, inner extraction well; FW103, outer extraction well. FW100, FW101, and FW102 are MLS wells. Symbols are located at the lateral position of the vertical center of the screened interval.

primarily to borehole deviation. A narrow fracture zone with high hydraulic conductivity was found at ~12-m depth, consistent with vertical profiles of chemical composition and electromagnetic borehole flowmeter testing, indicating that flow moves predominantly within this narrow region of preferential flow (Solomon et al. 1992; Fienen et al. 2004). The heterogeneity and difficulty in well alignment with regional flow motivated the four-well nested approach in this work.

We implemented a forced-gradient tracer test using the well system shown in Figure 10 to investigate its hydraulic performance. During the tracer tests, modified tap water was injected in the outer injection well FW024 at 141 L/h and into the inner injection well FW104 at 240 L/h. The inner extraction well FW026 pumped at 180 L/h, and the outer extraction well FW103 pumped at 84 L/h. To establish a steady-state flow field, a tracer-free acidified solution was injected over 18 h into both injection wells. Subsequently, an acidified solution containing $MgBr_2$ as tracer was injected into the inner injection well FW104 for 16 h, while a tracer-free acidified solution continued to be injected in the outer injection well FW024. After that, the tracer-free acidified solution was added again to both injection wells. The extraction wells were operated during all injection periods. The previous steps took 96 h in total. Finally, both the injection and extraction were stopped, reestablishing the ambient flow regime.

A nested inner cell was created between wells FW104 (injection) and FW026 (extraction), protected by outer cells created by wells FW024 and FW103. The total mass captured by the inner well FW026 was 55% of the total bromide injected, whereas 39% was captured by the outer well FW103. Only 6% of the mass was not recovered during the 96 h, indicating that the connection between the injection and extraction wells is acceptable. The unrecovered portion may be lost in the long tail of the breakthrough curve, removed during sampling at the MLS wells, or lost by leakage from the outer cell to regional flow. If the system were ideally homogeneous with wells placed exactly along strike and without transverse dispersion, the bromide mass captured by inner extraction well FW026 would equal the pumping rate ratio of 75% for the pumping rates used in the test. Both the misalignment of the wells and the heterogeneity of the aquifer led to the observed reduction of the recovery. Misalignment of the wells is equivalent to the regional flow orientation not parallel to the wells and may create a transitional zone between the inner and outer cells, resulting in tracer leakage from the inner to the outer cell. Heterogeneity may also provide some stream tubes directly connecting FW104 to FW103.

Figure 11 shows the breakthrough curves of nitrate at the outer extraction well FW103 and the MLS wells. The concentrations are normalized by the initial nitrate concentration. Since nitrate-free water was injected during the tracer test, the depletion in nitrate serves as an additional tracer. Nitrate concentrations at MLS wells FW101 and FW102 responded faster to the injection of nitrate-free water than MLS well FW100. Also, the levels at the former two wells dropped to very low values, <0.01, within the 4 d of injection. This difference in response is mainly due to variations in travel time. After pumping stopped, nitrate concentrations recovered to 60% to 95% of the initial value within 10 months. The rebound is caused by the intrusion of indigenous ground water and local mass transfer from immobile zones into the accessible mobile zone. This information confirms that the nested inner cell was almost completely separated from the intrusion of the regional flow during the tracer test. In addition, during the 4-d tracer test, the nitrate concentration in the outer extraction well FW103 dropped to 3% of the initial concentration, showing that most flow captured in the outer extraction well was from the injected clean water at wells FW024 and FW104.

Summary and Conclusions

Hydraulic control is a critical issue for in situ bioremediation. In contrast to pump-and-treat applications, multiple factors must be considered such as the

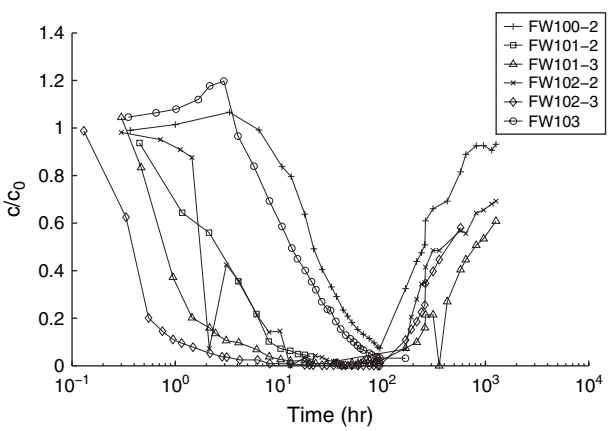

Figure 11. Normalized breakthrough curves of nitrate in the outer extraction well and the MLS wells during the tracer test. The extensions "-2" and "-3" denote the depths of 13.7 and 12.2 m below ground surface.

recirculation ratio, the area of the recirculation zones, and the residence time within. We first analyzed the hydraulics of a recirculation zone created by an extraction-injection well pair in arbitrarily oriented regional flow. We studied the impacts of the pumping rate and the regional flow orientation. New results include:

1. The recirculation ratio within the recirculation zone is sensitive to the regional flow direction, especially at low pumping rates.
2. The dimensionless area of the recirculation zone is approximately linear with the dimensionless pumping rate λ.
3. The average residence time within the recirculation zone approaches an asymptotic value at large λ. Once a well system is installed, it is almost impossible to adjust the average residence time within the recirculation zone by changing the pumping rate, at least for $\lambda > 20$.

We have presented an application at Oak Ridge, Tennessee, as a case study for in situ reactor design in which hydraulic control is of utmost importance. Here, we have proposed a four-well nested-cell approach. Compared to a two-well system, it has the following advantages:

1. The inner cell is separated from the regional flow by a protective outer cell.
2. The recirculation ratio in the nested inner cell is less sensitive than the two-well system to regional flow orientation.
3. The average residence time within the nested inner cell can easily be adjusted by changing the pumping rates of the wells.

A forced-gradient tracer test indicates stronger leakage from the inner to the outer cell than predicted for an idealized homogeneous aquifer. We believe such deviations are typical for most natural aquifers (Cirpka et al. 1999). The hydraulic design incorporates a margin of safety. If we had installed a classical two-well system, we would have mixed ambient flow into the proposed treatment zone and released water from the treatment zone to ambient flow. The current nested-cell design is less risky because the inner cell does not directly contact regional flow. Instead, there is an exchange between the inner and outer cells. Nonetheless, it is important to maintain favorable conditions by chemical amendments into both injection wells. In the ongoing bioremediation experiment, we add the electron donor only into the inner injection well, whereas the outer cell is flushed with a nitrate- and uranium-free solution at a pH that favors retention of sorbed U(VI). This minimizes loss of U(VI) from the system and creates favorable conditions for U(VI) reduction inside the inner cell.

Acknowledgments

This work was partially funded by the United States Department of Energy Natural and Accelerated Bioremediation Research Biological and Environmental Research grant #DE-F603-00ER63046. The authors appreciate the efforts of Paul Bayer, the NABIR program manager. We thank Dr. Jeffrey Cunningham, Dr. Hongbin Zhan, and Dr. David Hyndman for their helpful comments on the manuscript.

References

Abdelouas, A., Y. Lu, W. Lutze, and H.E. Nuttall. 1998. Reduction of U(VI) to U(IV) by indigenous bacteria in contaminated ground water. *Journal of Contaminant Hydrology* 35, no. 1–3: 217–233.

Brooks, S.C., J.K. Fredrickson, S.L. Carroll, D.W. Kennedy, J.M. Zachara, A.E. Plymale, S.D. Kelly, K.M. Kemner, and S. Fendorf. 2003. Inhibition of bacterial U(VI) reduction by calcium. *Environmental Science & Technology* 37, no. 9: 1850–1858.

Christ, J.A., M.N. Goltz, and J.Q. Huang. 1999. Development and application of an analytical model to aid design and implementation of in situ remediation technologies. *Journal of Contaminant Hydrology* 37, no. 3–4: 295–317.

Cirpka, O.A., E.O. Frind, and R. Helmig. 1999. Streamline-oriented grid generation for transport modelling in two-dimensional domains including wells. *Advances in Water Resources* 22, no. 7: 697–710.

Cunningham, J.A., T.P. Hoelen, G.D. Hopkins, C.A. Lebron, and M. Reinhard. 2004. Hydraulics of recirculating well pairs for ground water remediation. *Ground Water* 42, no. 6: 880–889.

Cunningham, J.A., and M. Reinhard. 2002. Injection-extraction treatment well pairs: An alternative to permeable reactive barriers. *Ground Water* 40, no. 6: 599–607.

Dybas, M.J., M. Barcelona, S. Bezborodnikov, S. Davies, L. Forney, O. Kawka, T. Mayotte, L. Sepveda-Torres, K. Smalla, M. Sneathen, J. Tiedje, T. Voice, D. Wiggert, M.E. Witt, and C.S. Criddle. 1998. Pilot-scale evaluation of bioaugmentation for *in situ* remediation of a carbon tetrachloride contaminated aquifer. *Environmental Science & Technology* 32, no. 22: 3598–3611.

Fienen, M.N., P.K. Kitanidis, D.B. Watson, and P.M. Jardine. 2004. An application of Bayesian inverse methods to vertical deconvolution of hydraulic conductivity in a heterogeneous aquifer at Oak Ridge National Laboratory. *Mathematical Geology* 36, no. 1: 101–126.

Finneran, K.T., M.E. Housewright, and D.R. Lovley. 2002. Multiple influences of nitrate on uranium solubility during bioremediation of uranium-contaminated subsurface sediments. *Environmental Microbiology* 4, no. 9: 510–516.

Gandhi, R.K., G.D. Hopkins, M.N. Goltz, S.M. Gorelick, and P.L. McCarty. 2002. Full-scale demonstration of *in situ* cometabolic biodegradation of trichloroethylene in ground water, 1: Dynamics of a recirculating well system. *Water Resources Research* 38, no. 4: 10.1029/2001WR000380.

Gorelick, S.M., R.A. Freeze, D. Donohue, and J.F. Keely. 1993. *Groundwater Contamination: Optimal Capture and Containment*. Boca Raton, Florida: CRC Press Inc.

Hyndman, D.W., M.J. Dybas, L. Forney, R. Heine, T. Mayotte, M.S. Phanikumar, G. Tatara, J. Tiedje, T. Voice, R. Wallace, D. Wiggert, X. Zhao, and C.S. Criddle. 2000. Hydraulic characterization and design of a full-scale biocurtain. *Ground Water* 38, no. 3: 462–474.

Luo, J., and P.K. Kitanidis. 2004. Fluid residence times within a recirculation zone created by an extraction-injection well pair. *Journal of Hydrology* 295, no. 1–4: 149–162.

McCarty, P.L., M.N. Goltz, G.D. Hopkins, M.E. Dolan, J.P. Allan, B.T. Kawakami, and T.J. Carrothers. 1998. Full-scale evaluation of *in situ* cometabolic degradation of trichloroethylene in ground water through toluene injection. *Environmental Science & Technology* 32, no. 1: 88–100.

Senko, J.M., J.D. Istok, J.M. Suflita, and L.R. Krumholz. 2002. In situ evidence for uranium immobilization and remobilization. *Environmental Science & Technology* 36, no. 7: 1491–1496.

Solomon, D.K., G.K. Moore, L.E. Toran, R.B. Dreier, and W.M. McMaster. 1992. A hydrologic framework for the Oak Ridge Reservation. ORNL/TM-12026. Publication 3815. Environmental Sciences Division, Oak Ridge National Laboratory.

Sturman, P.J., P.S. Stewart, A.B. Cunningham, E.J. Bouwer, and J.H. Wolfram. 1995. Engineering scale-up of in situ bioremediation processes: A review. *Journal of Contaminant Hydrology* 19, 171–203.

Witt, M.E., M.J. Dybas, D.C. Wiggert, and C.S. Criddle. 1999. Use of bioaugmentation for continuous removal of carbon tetrachloride in model aquifer columns. *Journal of Environmental Engineering Science* 16, no. 6: 475–485.

Zhan, H. 1999. Analytical and numerical modeling of a double well capture zone, *Mathematical Geology* 31, no. 2: 175–193.